ARTICLE

# Investigation on Binding between Cations and Amides using UV Raman Spectroscopy

Yi-xuan Liu[a], Zhou-bing Wang[a], Jing-jing Wang[a], Kang-zhen Tian[a,b], Xin Meng[a*], Gui-lin Mao[a,b*]

*a. School of Physics and Electronic Engineering, Jiangsu Normal University, Xuzhou 221116, China*
*b. Jiangsu Key Laboratory of Advanced Laser Materials and Devices, Xuzhou 221116, China*

(Dated: Received on January 18, 2023; Accepted on March 27, 2023)

The interaction of proteins with salt ions plays an important role in life activities. We used butyramide as a model molecule to investigate the interaction of protein backbones with cations. The experiment was performed in an aqueous solution of metal chloride using UV Raman spectroscopy. It was found that well-hydrated metal cations ($Ca^{2+}$, $Mg^{2+}$) tend to bind to C=O in the amide bond, resulting in redistribution of the amide I band peaks. Specifically, the peak intensity ratio of 1655 $cm^{-1}$ to 1610 $cm^{-1}$ increases significantly with increasing concentrations. However, this phenomenon is not obviously observed in NaCl solution. Furthermore, we studied the effect of salt ions on the water structures. The addition of $Ca^{2+}$ and $Mg^{2+}$ is beneficial to the enhancement of the water signal at the 3400 $cm^{-1}$ position, while the $Na^+$ at the same concentration is not obvious. The results have shown that the interaction between cations and amides satisfies the following order: $Ca^{2+}$>$Mg^{2+}$>$Na^+$, which conforms to the Hofmeister series.

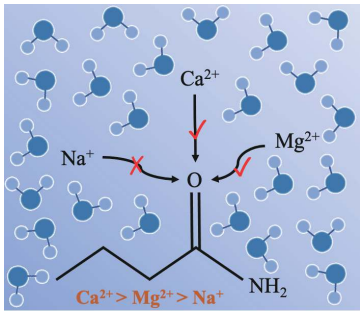


**Key words:** UV Raman spectroscopy, Butyramide, Hofmeister

## I. INTRODUCTION

Salt ions are commonly found in our surroundings and play an important role. For the study of salt ions, the law of salt ion and protein precipitation was discovered more than 100 years ago by Franz Hofmeister [1–3]. This law states that for a given cation, the effect of different anions on protein precipitation follows the following order [4, 5]:

$$CO_3^{2-} > SO_4^{2-} > S_2O_3^{2-} > H_2PO_4^- > F^- > Cl^- > Br^- \approx NO_3^- > I^- > ClO_4^- > SCN^-$$

The chloride ion is the critical ion. The ions on the left of the chloride ion can decrease protein solubility, causing protein to precipitate in solution and facilitating protein folding, which tends to make the protein more stable. The ions to the right of the chloride ion can increase protein solubility and promote protein dissolution into solution, leading to protein denaturation and thus reducing its stability. In addition, there is a similar sequence of cations [6, 7]:

$$Ca^{2+} > Mg^{2+} > Li^+ > Na^+ \approx K^+$$

Subsequent studies have revealed many phenomena about this unique salt ion sequence, including protein folding, protein crystallization, biological enzyme activity, colloid assembly, polymer collapse, and phase transition of phospholipid molecules. Therefore, the Hofmeister effect has been widely used in many fields [8–12] such as protein separation, electroanalytical chemistry, and the design of fouling-resistant materials.

By contrast to anions, the Hofmeister effect for

* Authors to whom correspondence should be addressed. E-mail: mengxin@jsnu.edu.cn, maoguilin@jsnu.edn.cn

 

cations is usually weaker [13]. There are many studies on anions [14–16], and cation–amide interactions are weaker in comparison to anion–amide, so the detection of cations is difficult. Current researches mainly focus on anionic sequences, due to the generally weak Hofmeister effect of cations. However, specific cation effects are of direct importance for protein folding, including protein interactions, cell signaling, protein aggregation, enzyme catalysis, and biotechnology [17–20]. Therefore, it is important to study the interactions of cations with the amide fraction and the peptide backbone.

Raman spectroscopy is a non-destructive, high-sensitivity measurement technique that is widely used in various fields such as physics, chemistry, biology, mineralogy, materials science, archaeology, and industrial product quality control [21–26]. It is a powerful tool for studying molecular structure and configuration. Raman spectroscopy measurements generally face two limitations. The first is the small Raman scattering cross section, which requires a strong laser and a sensitive detection system to obtain sufficient signals. The second is that the signal-to-noise ratio is further limited by the underlying inherent noise sources. The excitation light source used in ultraviolet Raman spectroscopy is located in the ultraviolet region. Since fluorescence mainly occurs in the visible region, shifting the excitation wavelength to the ultraviolet band can effectively avoid fluorescence interference. Light scattering intensity is inversely proportional to the fourth power of wavelength, and UV laser excitation can improve detection sensitivity. The electron absorption band of many substances is in the ultraviolet region, and ultraviolet resonance Raman spectroscopy can be performed, which improves the sensitivity of the instrument by several orders of magnitude. In addition, $H_2O$ is a relatively weak Raman scatterer, enabling Raman studies of biomolecules in water. Therefore, UV Raman spectroscopy has a wide range of applications in the field of biomedicine, detection of environmental pollutants, and detection of inorganic materials [27–31].

Therefore, we studied the interaction of salt ions with butyramide using UV Raman spectroscopy as a simple simulation of cation-protein backbone interactions. Because of the secondary structure of protein is often determined by its backbones, and its functional group is similar, so butyramide can be considered as the simplified version of protein backbones. The experiments were carried out in aqueous metal chloride solutions and it was found that the hydration of well-hydrated metal cations ($Ca^{2+}$, $Mg^{2+}$) makes the ratio $A_{1665}/A_{1610}$ increase. However, $Na^+$ does not have the same effect. Similarly, the addition of $Ca^{2+}$ and $Mg^{2+}$ favors the enhancement of the water signal at the 3400 $cm^{-1}$ position, while $Na^+$ is not significant.

## II. EXPERIMENTS AND METHODS

### A. Materials

The butyramide ($CH_3CH_2CH_2CONH_2$) was purchased from Sigma-Aldrich Co., Ltd. The salts of sodium chloride (NaCl), calcium chloride ($CaCl_2$), and magnesium chloride ($MgCl_2$) were purchased from Sinopharm Chemical Reagent Co., Ltd. with analysis purity. All the salts were baked for more than 6 h to remove the organic impurities. Ultra-pure water (with a resistivity of ≥18.2 MΩ•cm) was used in all experiments.

### B. Sample preparation

Place the weighed butylamine sample powder in a colorimetric dish, add 2 mL of pure water with a pipette, and then ultrasonically treat for 10 min to completely dissolve butylamine. with this method, 0.1, 0.7, 1.3, 1.9, 2.5, 3.1, 3.7, and 4.1 mol/L butyramide solutions were prepared. In the experiment of the interaction between butyramide and salt ions, three solid salt samples (NaCl, $CaCl_2$, $MgCl_2$) were added to 2 mol/L butyramide aqueous solution to make a series of 0.1, 0.7, 1.3, 1.9, 2.5, 3.1, 3.7, 4.1 mol/L butyramide mixed solutions, respectively; and sonicated to make solid salts fully dissolved. The dissolution state of the three salt ion aqueous solutions is similar, and there was no obvious precipitation.

### C. Raman measurement

The UV Raman spectroscopy system was a self-built equipment as shown in FIG. 1. It includes 266 nm laser, coupling lens, Raman probe, littrow structured dispersive UV spectrometer, computer, *etc.* The 266 nm excitation light source was converged to the end of the coupling mirror through the focusing lens, and entered the optical fiber through the coupling mirror. The Raman probe was close to the sample, and the Raman scattered light was induced and transmitted to the dispersion system. The grating inscription number was 3800 lines/mm, and the CCD detector was a Hamamatsu S10420 CCD array with a cooling type control cir-

DOI: 10.1063/1674-0068/cjcp2301008 

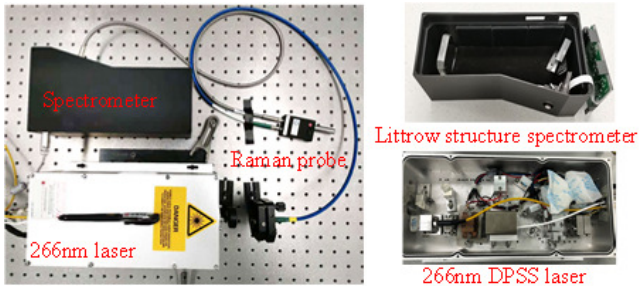


FIG. 1 The self-built UV Raman spectrometer.

cuit. The laser power was set to 180 mW and the spectrometer acquisition integration time was 10 s. During the test, the cuvette was placed in front of the Raman probe, and the position of the cuvette placement was adjusted by the strength of the Raman signal of the sample received by the spectrometer to ensure the maximum energy of the collected Raman spectrum. After the Raman spectral signal was stabilized, the Raman spectral signal was collected and saved.

## III. RESULTS AND DISCUSSION

### A. UV-Raman measurements of butyramide in powder and in solution

We tested the butyramide in powder as well as in solution to clarify the vibrational characteristic peaks. The results are shown in FIG. 2, and the Raman spectra were normalized in order to further distinguish the peak positions. It can be seen that the butyramide in powder state has more characteristic peaks. The characteristic peaks of butyramide in solution and in powder state can also correspond to each other. We concentrate on the amide vibration because the amide is the protein backbone structure. There are four different regions of amide, including the amide I spectral band, amide II spectral band, amide III spectral band, and amide A spectral band [27, 32, 33]. The amide I spectral band (~1660 $cm^{-1}$) comes mainly from C=O stretching vibrations and a few from heterophase C–N stretching vibrations. The amide II vibration (~1550 $cm^{-1}$), consists of a heterophasic combination of C–N stretching and N–H bending motions. Amide III (between ~1200 $cm^{-1}$ and 1340 $cm^{-1}$) spectral band is very complex, which is dominated by C–N stretching vibrations and N–H in-plane bending vibrations. The amide A spectral band locates in 3268–3274, 3278–3304, and 3355 $cm^{-1}$, which is used to analyze qualitatively the secondary structure of protein. We can see two peaks at 1615 $cm^{-1}$ and 1665 $cm^{-1}$ in aqueous solutions

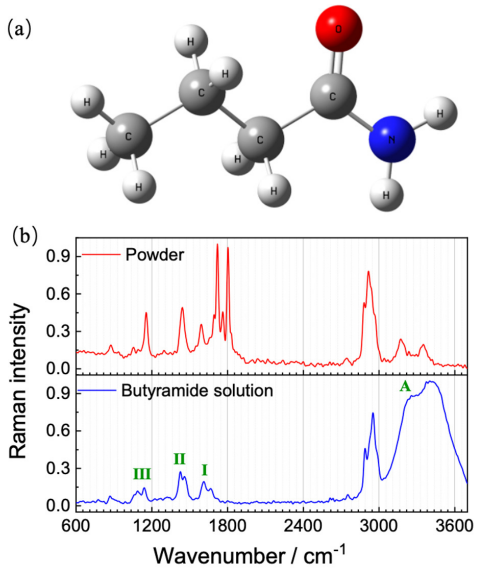


FIG. 2 (a) Molecular structure of butyramide. (b) Raman spectra of butyramide in powder and in solution.

of butyramide, attributed to the amide I spectrum band. Amide II and amide III vibrations are not observed. In addition, we can detect significant peaks at 1155 $cm^{-1}$ (C–C stretching), 1440 $cm^{-1}$ (N–C=O stretching), 1720 $cm^{-1}$ (C=O stretching), 1762 $cm^{-1}$ (C=O stretching), 1803 $cm^{-1}$ (C=O stretching), 2890 $cm^{-1}$ and 2917 $cm^{-1}$ ($CH_3$ stretching). We can observe two vibrational peaks of the water, located at ~3200 $cm^{-1}$ and ~3400 $cm^{-1}$, attributed to the amide A spectral band. This is because the O–H stretching band of $H_2O$ overlaps seriously with the amide A band. These characteristic peaks have a good signal-to-noise ratio and can be used as an effective support for their structure.

### B. UV-Raman measurements of the interaction of butyramide with NaCl, $CaCl_2$, and $MgCl_2$

Firstly, we investigated the structure of butylamine in solutions with different concentration. It can be seen that as the concentration increases, the signal of butyramide appears to grow significantly, as shown in FIG. 3(a-1). Considering that the amide I band can indicate the state in which the butyramide is located, we fitted two sign peaks of the amide I band at 1610 $cm^{-1}$ and 1665 $cm^{-1}$ to study the variation of its ratio with concentration. It can be seen that as the concentration increases, the ratio $A_{1655/1610}$ stabilizes at ~0.55 and does not change significantly. This suggests that the increase in Raman signal is only caused by volume changes and not by new structures or new interactions

DOI: 10.1063/1674-0068/cjcp2301008 

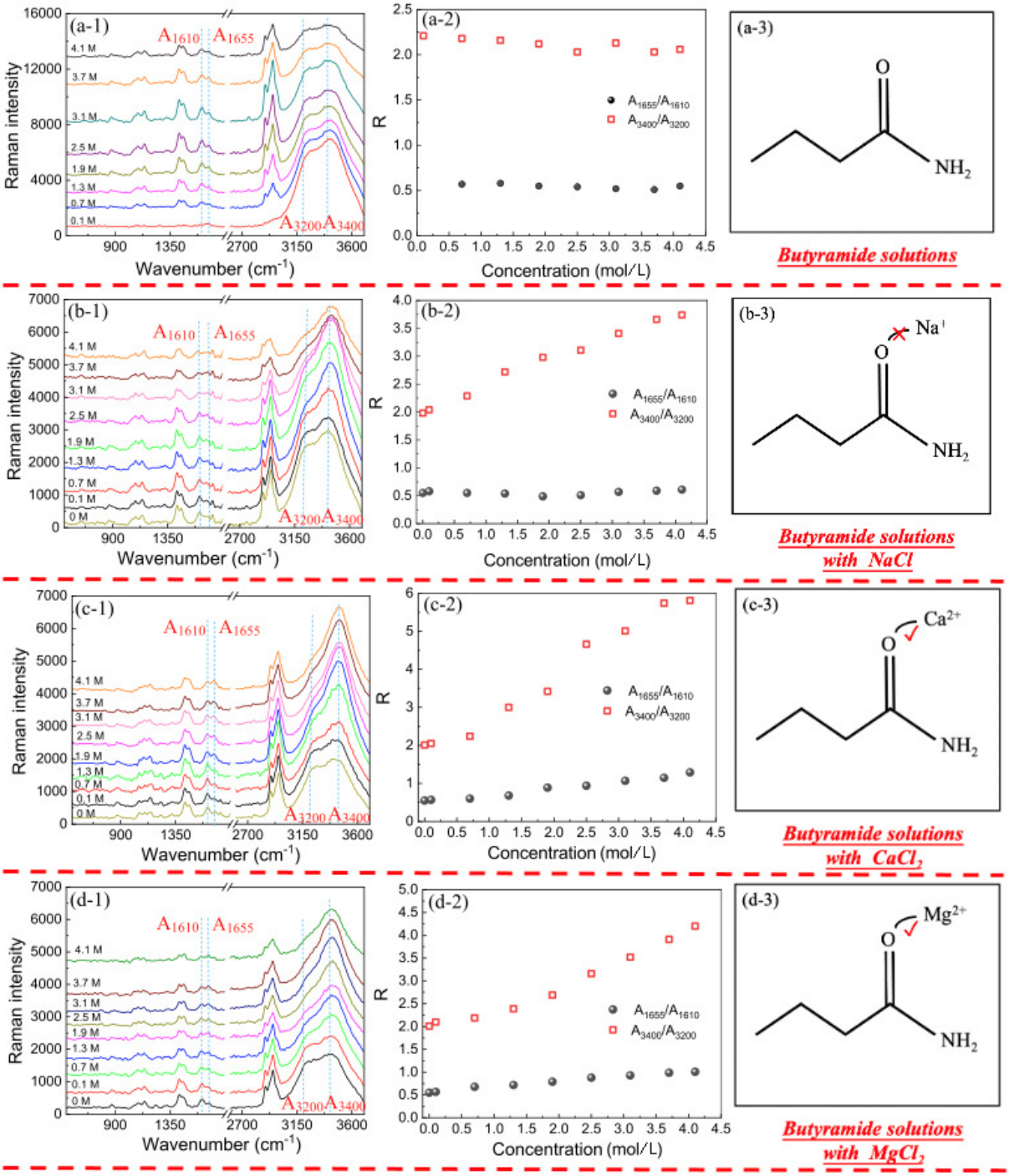


FIG. 3 UV-Raman measurements of the interaction of butyramide with different solutions. From left to right are Raman spectra, the ratio of $A_{1655/1610}$ and $A_{3400/3200}$, and schematic representation of butyramide molecule with different cations. (a) Butyramide solutions. (b) Butyramide with NaCl. (c) Butyramide with $CaCl_2$. (d) Butyramide with $MgCl_2$.

of the production type. The structural changes of the amide band are closely related to the structure of water. We further fitted the two peaks ~3200 $cm^{-1}$ and ~3400 $cm^{-1}$ and gave the ratio of the two peaks as a function of concentration, as shown in FIG. 3(a-2). These two vibrational peaks at ~3200 $cm^{-1}$ and ~3400 $cm^{-1}$ are suggested to originate from the ice-like structure and water-like structure of water molecules, respectively [34]. However, it has been reported that they are derived from the splitting of the symmetric stretching vibration of the water molecule and the Fermi resonance of the bending vibration multiples [35]. In short, the peaks at ~3200 $cm^{-1}$ and ~3400 $cm^{-1}$ are the strongly bound DDAA and the weakly bound DDAA

DOI: 10.1063/1674-0068/cjcp2301008 

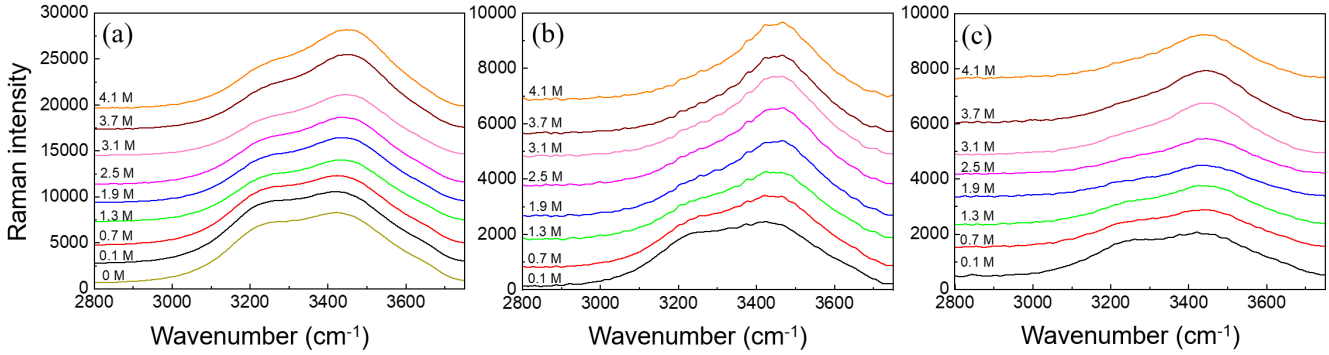


FIG. 4 Raman spectra of different salt solutions: (a) NaCl solutions, (b) $CaCl_2$ solutions and (c) $MgCl_2$ solutions.

molecules, where D and A denote the hydrogen bonds that provide and receive protons, respectively [36]. We can see that the intensity ratio of the peak at 3400 $cm^{-1}$ to that at 3200 $cm^{-1}$ is stable at ~2 and does not change significantly with the butyramide concentration.

Then, we investigated the interaction of salt ions with butyramide. The first chosen salt was NaCl. As can be seen from FIG. 3(b-1), the butyramide Raman signal ratio $A_{1655/1610}$ is basically stable at 0.55 for NaCl concentrations in the range of 0.1–2.5 mol/L. When the concentration is greater than 2.5 mol/L, the ratio has a slight increase to ~0.6. In contrast, the change in the water signal is more pronounced. The peak intensity ratio of water at 3400 $cm^{-1}$ to 3200 $cm^{-1}$ increases with the NaCl concentration from ~2 mol/L to ~3.7 mol/L, as shown in FIG. 3(b-2). This indicates that the addition of salt ions causes a change in the water structure. However, the interaction of sodium ions in NaCl with butyramide is weak and almost undetectable.

In comparison, the effect of calcium chloride solution on the structure of butyramide is more obvious. It can be seen from FIG. 3(c-1) and FIG. 3(c-2) that the intensity of the peak increases significantly at 1665 $cm^{-1}$ compared to 1610 $cm^{-1}$. The ratio $A_{1655/1610}$ increases from ~0.55 to ~1.3 with increasing concentration. The corresponding change in water is also more obvious. It can be seen that the peak at 3400 $cm^{-1}$ has significant increase. The ratio $A_{3400/3200}$ increases from 2 to ~6. This indicates a more pronounced interaction of calcium ions with butyramide. The calcium ion is positively charged and readily interacts with the C=O bond, which affects the coupling of the C=O stretching vibration and the C–N stretching vibration. Thus, the proportional reproduction assignment of the amide I spectral band appears.

Magnesium ions are similar in nature to calcium ions, and the peak intensity ratio of 1655 $cm^{-1}$ to 1610 $cm^{-1}$ has significant increase with concentration increase. As shown in FIG. 3(d-1) and FIG. 3(d-2), $A_{1655/1610}$ is raised from ~0.55 to ~1. Correspondingly, the water of 3400 $cm^{-1}$ has a clear advantage in the structure. Its ratio of $A_{3400/3200}$ improves from ~2 to ~4. This indicates that magnesium ion is similar to calcium ion. It is able to interact with the amide bond. Its ability to act is weaker than calcium ion, but significantly stronger than sodium ion.

### C. UV-Raman spectra of water in different concentrations of NaCl, $CaCl_2$, and $MgCl_2$ solution

In order to understand the mechanism of the interaction between salt ions and butyramide, we further investigated the effect of salt ions on the water structure. As shown in FIG. 4, for the NaCl solution, two distinct peaks can be observed in the range of 3200 $cm^{-1}$ to 3400 $cm^{-1}$. As the concentration increases, the distribution of 3200 $cm^{-1}$ and 3400 $cm^{-1}$ remains constant at low concentrations. When the concentration is higher than 2.5 mol/L, the 3400 $cm^{-1}$ partition increases slightly. For calcium chloride and magnesium chloride solutions, the relative intensity of 3200 $cm^{-1}$ decreases with increasing concentration, while the relative intensity of 3400 $cm^{-1}$ increases significantly. This indicates that only calcium and magnesium ions have a significant effect on the structure of water.

In salt soltuion of butyramide, the driving force of the cation-peptide interaction involves electrostatic interactions between the cation and the amide. Cations tend to gravitate closer to C=O. This effect is very weak and can be clearly observed only at high concentrations. This difference in the Hofmeister series can be understood on the basis of the very different binding sites for cations and anions. Thus, the amide oxygen is the key binding site for the cation.

DOI: 10.1063/1674-0068/cjcp2301008 

## IV. CONCLUSION

In this study, we established an experimental protocol based on UV-Raman to study the interaction of salt ions with butyramide. We mainly studied $Na^+$, $Ca^{2+}$, and $Mg^{2+}$ in the Hofmeister cation series. It was found that $Ca^{2+}$ and $Mg^{2+}$ tend to bind to C=O in the amide bond, leading to the redistribution of the amide I band peaks. At the same time, the water signal at the 3400 $cm^{-1}$ position is enhanced. Under the same conditions, the effect of $Na^+$ is not obvious. At the same time, the hydration is also related to the combination of other amide structures, which provides a basis for the establishment of a relationship between hydration and Hofmeister effect to a certain extent. This is in accordance with the pattern of the Hofmeister series. The special capabilities of our method will be able to provide important clues to study the safety of salt ion-protein interactions.

## V. ACKNOWLEDGEMENTS

This work was supported by the National Natural Science Foundation of China (No.62005108, No.62205134), the Natural Science Foundation of the Higher Education Institutions of Jiangsu Province (No.21KJB140008), and the Graduate Research and Practice Innovation Program of Jiangsu Normal University (No.2021XKT1201, No.2021XKT1204).

[1] A. Mukhopadhyay and P. Dubey, J. Raman Spectrosc. **49**, 736 (2018).
[2] B. C. Gibb, Nat. Chem. **11**, 963 (2019).
[3] J. Tang, Nat. Nanotechnol. **14**, 1091 (2019).
[4] K. P. Gregory, G. R. Elliott, H. Robertson, A. Kumar, E. J. Wanless, G. B. Webber, V. S. J. Craig, G. G. Andersson, and A. J. Page, Phys. Chem. Chem. Phys. **24**, 12682 (2022).
[5] B. Rana, D. J. Fairhurst, and K. C. Jena, J. Am. Chem. Soc. **144**, 17832 (2022).
[6] M. Lalic, A. AnticJovanovic, M. Jeremic, S. Sasic, Spectrosc. Lett. **29**, 267 (1996).
[7] S. Cruz-Leon and N. Schwierz, Langmuir **36**, 5979 (2020).
[8] P. H. C. Paiva, Y. L. Coelho, L. H. M. da Silva, M. S. Pinto, M. C. T. Vidigal, and A. C. D. S. Pires, Food Chem. **305**, 125463 (2020).
[9] S. S. Ribeiro, T. G. Castro, C. M. Gomes, and J. C. Marcos, Phys. Chem. Chem. Phys. **23**, 25210 (2021).
[10] B. C. Gibb, Nat. Chem. **10**, 797 (2018).
[11] J. H. Jordan, C. L. D. Gibb, A. Wishard, T. Pham, and B. C. Gibb, J. Am. Chem. Soc. **140**, 4092 (2018).
[12] W. Wei, X. Chen, and X. Wang, Small **18**, 2200921 (2022).
[13] H. I. Okur, J. Kherb, and P. S. Cremer, J. Am. Chem. Soc. **135**, 5062 (2013).
[14] Y. Zhang and P. S. Cremer, Annu. Rev. Phys. Chem. **61**, 63 (2010).
[15] K. D. Collins, G. W. Neilson, J. E. Enderby, Biophys. Chem. **128**, 95 (2007).
[16] P. Jungwirth and B. Winter, Rev. Phys. Chem. **59**, 343 (2008).
[17] Y. An, K. Sun, Y. Qiu, and L. Zhang, Minerals **12**, 1070 (2022).
[18] M. R. Fries, N. F. Conzelmann, L. Guenter, and O. Matsarskaia, M. W. Skoda, R. M. Jacobs, and F. Schreiber, Langmuir **37**, 139 (2021).
[19] A. Kato, Y. Katsuki, and E. Nishimoto, Chem. Phys. Lett. **730**, 89 (2019).
[20] M. E. Richert, G. G. Gochev, and B. Braunschweig, Langmuir **35**, 11299 (2019).
[21] K. Tian, W. Wang, Y. Yao, X. Nie, A. Lu, Y. Wu, and C. Han, J. Raman Spectrosc. **49**, 472 (2018).
[22] M. Arabi, A. Ostovan, Z. Zhang, Y. Wang, M. Arabi, A. Ostovan, Z. Zhang, Y. Wang, R. Mei, L. Fu, and L. Chen, Biosens. Bioelectron. **174**, 112825 (2021).
[23] F. Nicolson, M. F. Kircher, N. Stone, and P. Matousek, Chem. Soc. Rev. **50**, 556 (2021).
[24] P. Shvets, O. Dikaya, K. Maksimova, and A. Goikhman, J. Raman Spectrosc. **50**, 1226 (2019).
[25] J. F. Schultz, S. Mahapatra, L. Li, and N. Jiang, Appl. Spectrosc. **74**, 1313 (2020).
[26] J. Wang, K. Liu, S. Jin, L. Jiang, and P. Liangg, Appl. Spectrosc. **74**, 130 (2020).
[27] S. A. Oladepo, K. Xiong, Z. Hong, S. A. Asher, J. Handen, and I. K. Lednev, Chem. Rev. **112**, 2604 (2012).
[28] J. Geng, M. Aioub, M. A. El-Sayed, and B. A. Barry, ChemPhysChem **19**, 1428 (2018).
[29] M. Liu, Y. Shi, M. Wu, Y. Tian, H. Wei, Q. Sun, and B. Man, J. Raman Spectrosc. **51**, 750 (2020).
[30] P. Ortiz-Amezcua, A. Esteban Bedoya-Velasquez, J. A. Benavent-Oltra, D. Pérez-Ramírez, I. Veselovskii, M. Castro-Santiago, and L. Alados-Arboledas, Opt. Express **28**, 8156 (2020).
[31] B. W. Lin, Y. H. Tai, Y. C. Lee, D. Xing, H. C. Lin, H. Yamahara, and J. J. Delaunay, Appl. Phys. Lett. **120**, 051102 (2022).
[32] Y. Gao, T. Xuan, F. Chen, Y. Wu, X. Guo, Y. Wen, and H. Yang, Sens. Actuators B **304**, 127223 (2020).
[33] S. C. Epstein, A. R. Huff, E. S. Winesett, C. H. Londergan, and L. K. Charkoudian, Nat. Commun. **10**, 2227 (2019).
[34] Y. R. Shen and V. Ostroverkhov, Chem. Rev. **106**, 1140 (2006).
[35] M. Sovago, R. K. Campen, G. W. H. Wurpel, M. Müller, H. J. Bakker, and M. Bonn, Phys. Rev. Lett. **100**, 173901 (2008).
[36] S. Ye, S. Ma, F. Wei, and H. Li, Analyst **137**, 4981 (2012).

DOI: 10.1063/1674-0068/cjcp2301008 